

Real-space tight-binding approach to stability and order in substitutional multicomponent alloys

P. E. A. Turchi

Lawrence Livermore National Laboratory, L-268, P.O. Box 808, Livermore, California 94551

D. Mayou and J. P. Julien

LEPES-CNRS, 25 Avenue des Martyrs, Boite Postale 166, F-38042 Grenoble Cedex 9, France

(Received 26 March 1997)

A real-space approach based on the tight-binding approximation for studying electronic structure properties and stability and order in substitutional multicomponent alloys is presented. First, for a chemically random alloy based on a periodic lattice, we show that the coherent potential approximation equations can be solved self-consistently in real space with the same accuracy currently achieved in reciprocal space. The resulting one-electron Green function is given by a continued fraction expansion, and this analytic form can be conveniently used to determine alloy properties, and in particular the energetics. Second, combined with an orbital-peeling technique, this method allows in a very efficient way the calculation of the effective cluster interactions which enter the expression of the configurational part of the total energy for describing order-disorder phenomena in alloys. Finally, we present some applications and briefly discuss the possible extensions of this approach. [S0163-1829(97)07028-8]

I. INTRODUCTION

It has long been recognized that order-disorder phenomena and structural transformations affect a majority of the physical properties exhibited by most alloys as functions of temperature, pressure, and concentration. Models based on electronic structure calculations have been developed to predict chemical order in alloys, and their effect on alloy properties.¹ More recently, with the discovery of bulk amorphous alloys, more precise experiments are being performed to provide a better understanding of how chemical order, and in particular short-range order, can affect the final topology adopted by an alloy, and consequently alloy properties. In this context, there is a need to develop efficient electronic structure models entirely solvable in real space which are capable of accounting for chemical order effects in materials with reduced or no symmetry.

For pure elements or alloys which are characterized by fairly localized electrons, such as transition metals and their alloys, or by covalent bonding, such as C, Si, and Ge, the tight-binding approximation (TBA) allows a fairly accurate description of their electronic structure properties. Since the 70's, real-space techniques, and in particular the recursion method,^{2,3} have been widely used within the TBA. One major advantage of this latter method, besides its numerical stability, resides in the fact that the one-electron Green function is expressed in terms of a continued fraction expansion. The asymptotic behavior of the coefficients of the continued fraction as a function of the characteristics of the support of the electronic spectrum is now well known, and the termination of the truncated continued fraction can be performed at ease.⁴ The other obvious advantage is that the electronic structure of systems with reduced symmetry, such as in the presence of extended defects, e.g., dislocations, grain boundaries, interfaces, or surfaces, or with no periodicity at all, as in the case of amorphous alloys, can be conveniently investigated by real-space approaches. However, the success of

TB-based studies crucially depends on a reliable determination of the parameters which describe both the TB electronic Hamiltonian and the energetics. Although no systematic procedure to generate these parameters exists at present, methods such as the TB version of the linear muffin-tin orbital (LMTO) method⁵ allow a direct determination of the hopping integrals $\beta_{nm}^{\lambda\mu}$ in terms of Slater-Koster parameters, and of the on-site energies $\epsilon_{n\lambda}$ (or crystal field integrals), which enter the TB Hamiltonian given by

$$H = \sum_{n,\lambda} |n\lambda\rangle \epsilon_{n\lambda} \langle n\lambda| + \sum_{\substack{n,m \neq n \\ \lambda,\mu}} |n\lambda\rangle \beta_{nm}^{\lambda\mu} \langle m\mu|, \quad (1.1)$$

where n and m refer to site indices, and λ and μ to orbitals (for example, $\lambda, \mu = 1, 9$ in the case of systems characterized by *spd* electrons).

In recent years methods have been developed to cast the quantum mechanical description of the energetics of an alloy in the form of an Ising model which is most appropriate for a subsequent statistical mechanics treatment of order-disorder phenomena in alloys as functions of temperature and concentration.¹ The mapping of the energetics resulting from the solution of the Hamiltonian H , for example given by Eq. (1.1), onto an Ising form has been originally achieved within the so-called generalized perturbation method (GPM).⁶ The GPM is a perturbation treatment applied to a reference medium which is close to any chemical configuration of the alloy. Intuitively, the appropriate medium to use is the completely disordered state, as the one described within the coherent potential approximation (CPA).⁷⁻⁹ Subsequently, the method has been generalized to account for the correlations inside finite clusters embedded in the CPA-reference medium, thus leading to the so-called embedded cluster method (ECM).¹⁰ In both methods, only the configuration-dependent contribution to the total energy is expressed by an expansion in terms of effective pair and multisite interactions, and since the reference medium is con-

centration dependent, so are these interactions. One should emphasize that these two methods are in contrast with those based on the knowledge of the electronic structure properties of ordered configurations of the alloy, such as the so-called Connolly-Williams method,¹¹ which lead to an expansion of the total energy itself in terms of cluster interactions which are concentration independent, except via volume effects. Within the ECM, the configurational (or ordering) energy for a binary alloy is given by

$$\Delta E_{\text{ord}}(\{p_n\}) = \sum_n V_n^{(1)} \delta c_n + \sum_{n,m \neq n} V_{nm}^{(2)} \delta c_n \delta c_m + \dots \quad (1.2)$$

where δc_n refers to the fluctuation of concentration on site n , $\delta c_n = p_n - c$, where c is the concentration in B species, and p_n is an occupation number associated with site n , equal to 1 or 0 depending on whether or not site n is occupied by a B species. The $V^{(\alpha)}$ are the effective interactions involving clusters of α sites.

Once these interactions are known, the ground-state properties of the alloy at zero-temperature, i.e., the possible ordered state which is stable at each concentration, can be predicted. Finally, combined with a statistical model such as the cluster variation method or with Monte Carlo simulations, the configurational part of the free energy can be computed, and hence, the phase diagram of an alloy which summarizes the phase stability properties as functions of temperature and concentration.¹ With this motivation in mind, we show that the effective interactions can be easily calculated in real space using the so-called orbital-peeling method first introduced by Burke,¹² based on the solution of the CPA equations. The application of the real-space extended recursion technique to obtain these solutions is one of the subjects discussed in this paper.

So far, most studies on stability and order in alloys have been performed for alloys based on simple periodic lattices. Within the present real-space approach, it will be possible to extend such studies to alloys based on complex lattices even in the presence of extended defects, as well as to topologically (structurally) disordered materials.

The rest of the paper is organized as follows. In Sec. II, after a brief introduction of the CPA equations in the locator formalism, we present the principle of the solution of these equations in real space, and then some technical aspects of the new approach. Then we relate the so-called sum space in which the CPA-extended recursion is performed to the augmented space introduced by Mookerjee,^{13,14} and give some of its properties. Finally we show how to calculate the coefficients of the continued fraction expansions of the CPA self-energy and renormalized interactor for binary and higher-order multicomponent alloys. In Sec. III, we briefly review the formalism which leads to the ECM, and the implementation of the orbital-peeling method for calculating the effective interactions which build up the configurational part of the total energy of an alloy within this ECM. In Sec. IV, some applications of this real-space approach are discussed. In particular, the density of states and the effective interactions for binary, pseudobinary, and ternary transition metal alloys as obtained with the real-space approach are compared with the ones calculated with the well known k -space meth-

odology. Finally, in Sec. V, we summarize our results, and briefly discuss the possible extension of this method to study more complex alloy situations.

II. REAL-SPACE SOLUTION OF THE CPA EQUATIONS

In this section we show how the self-consistent CPA equations which describe chemical disorder in substitutional alloys are solved within the real-space method presented in this work. To this end, we begin by recalling briefly the classical formulation of the CPA equations in the locator formalism which is most convenient for introducing our method. Then, in the following three subsections we present the new formalism. Finally we give a summary of the method and discuss how this approach is extended to the multiband case, which is a requirement for studying the electronic structure properties of realistic alloy systems.

A. The CPA equations

For the sake of clarity, let us first consider the case of a binary alloy with only one s orbital located on each site of its underlying lattice. The generalization to multiband alloys is straightforward, and will be discussed in the summary of this section. Since we only consider (for now) the case of diagonal disorder, the Hamiltonian H for a given configuration of the alloy is written in the form

$$H = H_0 + V, \quad (2.1)$$

where H_0 is the site off-diagonal part of the Hamiltonian which is supposed to be independent of disorder, and is written in terms of the hopping integrals β_{nm} between sites n and m as

$$H_0 = \sum_{n,m \neq n} \beta_{nm} |n\rangle \langle m|, \quad (2.2)$$

and V is the random diagonal part of H given by

$$V = \sum_n \epsilon_n |n\rangle \langle n|, \quad (2.3)$$

where

$$\epsilon_n = \sum_i p_n^i \epsilon_n^i \quad (2.4)$$

and $|n\rangle$ is an atomic orbital (here, there is one orbital per site) centered on site n , p_n^i is equal to one if site n is occupied by the atomic species i and to zero otherwise, and ϵ_n^i is the on-site energy associated with species i centered on site n (unless otherwise specified, we will assume in the following that this quantity, referred to as ϵ_i , does not depend on n). In the following we will also assume that the atomic orbitals form an orthonormal basis, i.e., $\langle n|m\rangle = \delta_{nm}$, where δ_{nm} is the usual Kroenecker symbol.

In order to introduce our new methodology, it is convenient to start from the locator equation of motion for a site-diagonal element of the Green function^{9,15} which takes the form

$$G_{nn} = g_n + g_n \Delta_n G_{nn}, \quad (2.5)$$

where g_n is the locator associated with site n , given by $(z - \epsilon_n)^{-1}$, and

$$\Delta_n = \sum_{m \neq n} \beta_{nm} g_m \beta_{mn} + \sum_{\substack{m \neq n \\ l \neq m}} \beta_{nl} g_l \beta_{lm} g_m \beta_{mn} + \dots \quad (2.6)$$

This quantity, Δ_n , represents the change in energy of an electron at site n due to its interaction with the surrounding medium. Note that in the case of diagonal disorder only, Δ_n depends on the configuration of the medium surrounding site n , but not on the occupation of the site n itself. The Green function can be rewritten as

$$G_{nn} = (g_n^{-1} - \Delta_n)^{-1} = (z - \epsilon_n - \Delta_n)^{-1}. \quad (2.7)$$

In agreement with the assumptions behind the single-site CPA, the average medium surrounding site n is assumed to be given by a Hamiltonian with a site-diagonal coherent potential σ which is a function of the complex energy z , and off-diagonal elements given in terms of the hopping integrals β . The expression for $\bar{\Delta}$ associated with this average medium is given by an expression analogous to Eq. (2.6) but with each g_n replaced by $\bar{g} = (z - \sigma)^{-1}$, the so-called bare locator for the effective medium. Therefore, we obtain an approximation for the site-diagonal element G_{00}^i associated with an atom of type i (here, $i = A$ or B) at site 0 embedded in the medium:

$$G_{00}^i = (z - \epsilon_i - \bar{\Delta}_0)^{-1}. \quad (2.8)$$

Due to the independence of $\bar{\Delta}_0$ on the occupation of site 0, the site-diagonal element of the Green function associated with the effective medium is given by

$$\bar{G}_{00} = (z - \sigma - \bar{\Delta}_0)^{-1}. \quad (2.9)$$

Within the CPA, the self-energy σ is determined through the self-consistency condition

$$\langle G_{00}^i \rangle = \bar{G}_{00}, \quad (2.10)$$

that is,

$$\sum_i c_i (z - \epsilon_i - \bar{\Delta}_0)^{-1} = (z - \sigma - \bar{\Delta}_0)^{-1} = G_{\text{eff}}(z), \quad (2.11)$$

where c_i is the concentration in i species.

This implicit equation for σ is usually solved numerically at each complex energy z , for either the single or the multi-orbital case. Making use of the fact that the average medium has the periodicity of the underlying lattice, this solution is effected in reciprocal space within the propagator formalism, using the Bloch's theorem. It is well known that the CPA condition in the locator formalism is identical to the corresponding condition in the propagator formalism as well as in the mean-field approach⁸ which are most commonly used for the solution of the CPA equations. Note that in reciprocal space, the standard numerical approach requires a diagonalization of the Hamiltonian until full convergence of the solution to the CPA equations is achieved at each energy step and each \mathbf{k} point. In practice, this mode of operation

imposes drastic constraints on memory allocation and time of execution. We will show in the following that our real-space approach is free of these limitations, and opens up the possibility of addressing more complex issues than those possible with presently available techniques.

B. Principle of the real-space methodology

In the following we present a real-space solution of the CPA equations which employs the two self-energies: $\sigma(z)$, which represents the effect of chemical disorder, and $\Delta_n(z)$, the so-called renormalized interactor, associated with site n , which accounts for the coupling between site n and the surrounding medium, here the effective medium as described within the CPA. From Eq. (2.6), it is clear that the interactor that we now denote $\Delta(z)$ depends on the effective medium which is entirely defined by $\sigma(z)$. Thus, we can formally write the functional relation

$$\Delta(z) = f[\sigma(z)]. \quad (2.12)$$

Then, the CPA self-consistency condition can be expressed as

$$\sigma(z) = g[\Delta(z)], \quad (2.13)$$

which leads to an iterative solution for $\sigma(z)$ at each complex energy z .

Since the two basic functions $\Delta(z)$ and $\sigma(z)$ are Herglotz (which can be rigorously proved), they can be represented by continued fractions, and in the following we will use the notations

$$\sigma(z) = A_0 + \frac{B_1^2}{z - A_1 - \frac{B_2^2}{z - A_2 - \frac{B_3^2}{z - \dots}}} \quad (2.14)$$

and

$$\Delta(z) = \frac{b_1^2}{z - a_1 - \frac{b_2^2}{z - a_2 - \frac{b_3^2}{z - \dots}}}. \quad (2.15)$$

Thus, the basic principle of our method is to determine the continued fraction coefficients $\{A_p, B_p\}$ for σ and $\{a_q, b_q\}$ for Δ , rather than calculating σ and Δ at each complex energy z .

To avoid the introduction of additional functions or operators, we will constantly use in the following the equivalence between the continued fraction expansion of $\sigma(z)$ [or $\Delta(z)$] and the schematic representation of the associated TB Hamiltonian by a semilinear chain whose on-site energies are the A_q (or a_p) and the nearest-neighbor hopping integrals are the B_q (or b_p), as indicated in Fig. 1. This equivalence immediately allows us to replace the effective Hamiltonian $H_{\text{eff}}(z)$ for the disordered alloy by a Hamiltonian represented by the semilinear chain (A_q, B_q) attached to each site of the lattice on which the alloy is based. These chains exactly represent the effect of the self-energy $\sigma(z)$. This second equivalence is represented in Fig. 2 in the case of an alloy based on an infinite linear chain. With this energy-independent effective Hamiltonian, associated with the semi-

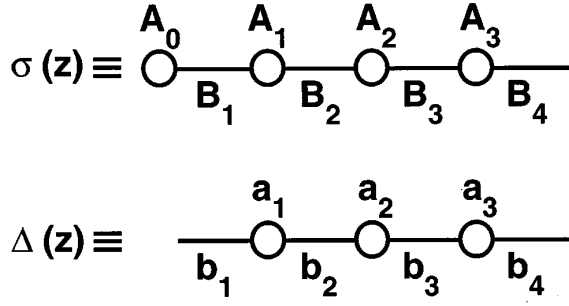


FIG. 1. Schematic representation of the continued fraction expansion of the self-energy $\sigma(z)$ and of the renormalized interactor $\Delta(z)$ by semilinear chains.

linear chain, the matrix element of the Green function can be calculated. The advantage of this formulation resides in the fact that methods developed for solving TB Hamiltonians, such as the recursion technique, can now be used. If one calculates $\Delta(z)$ by a recursion method with an initial recursion vector $|0\rangle$ which is taken to be the atomic orbital $|0\rangle$ centered on site 0, then it is well known that the successive vectors $|p\rangle$ of the recursion extend away from site 0. In particular, $|p\rangle$ will have nonzero components on sites q of the chain attached to the sites of the real crystal up to a finite value of q . Thus, in order to calculate $|p\rangle$ and also (a_p, b_p) , we do not need to know all the (A_q, B_q) . It is shown later by a precise analysis of the recursion scheme that one can obtain an expression for the a_p and b_p in terms of the (A_q, B_q) of the following type:

$$\begin{aligned} a_p &= a_p(A_{p-1}, B_{p-1}, \dots, B_1, A_0), \\ b_p &= b_p(B_{p-1}, A_{p-2}, \dots, B_1, A_0), \end{aligned} \quad (2.16)$$

which is another way of expressing Eq. (2.12).

Let us for now reconsider the self-consistent CPA equation (2.11), and show how to get information on the A_q and B_q from the (a_p, b_p) . A Laurent's expansion of both sides of this equation expressed as

$$\begin{aligned} \mu(2p) &= \mu(B_p, A_{p-1}, B_{p-1}, \dots, A_0; b_p, a_{p-1}, b_{p-1}, \dots, b_1), \\ \mu(2p+1) &= \mu(A_p, B_p, A_{p-1}, B_{p-1}, \dots, A_0; a_p, b_p, a_{p-1}, b_{p-1}, \dots, b_1). \end{aligned} \quad (2.20)$$

Thus, by using Eq. (2.18) we can calculate, at least in principle, the coefficients A_q and B_q from the coefficients a_p and b_p . One easily gets

$$\begin{aligned} A_0 &= A_0(\{\epsilon_i\}), \\ B_1 &= B_1(b_1), \\ A_1 &= A_1(a_1, b_1) \\ B_2 &= B_2(b_2, a_1, b_1), \end{aligned} \quad (2.21)$$

and for the general terms

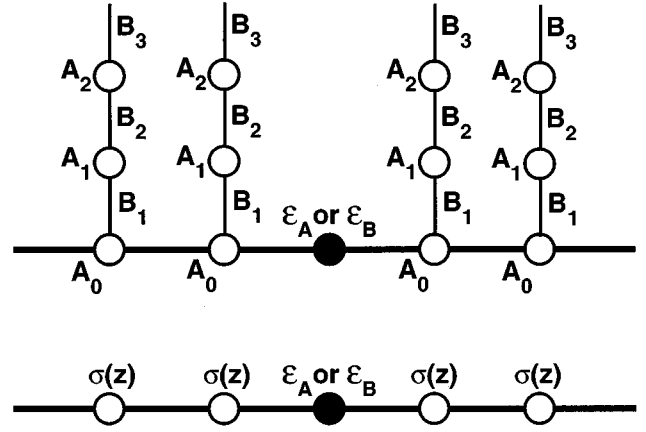


FIG. 2. Equivalent representations of the effective Hamiltonian describing chemical disorder, within the CPA, here for an alloy based on an infinite linear chain (thick solid lines).

$$\begin{aligned} \frac{1}{z - \epsilon_i - \bar{\Delta}(z)} &= \sum_p \frac{\mu_i(p)}{z^{p+1}}, \\ \frac{1}{z - \sigma(z) - \bar{\Delta}(z)} &= \sum_p \frac{\mu(p)}{z^{p+1}}, \end{aligned} \quad (2.17)$$

gives by identification of the terms associated with the same power of $1/z$ the result

$$\mu(p) = \sum_i c_i \mu_i(p) \quad (2.18)$$

for $p \geq 0$. Then, recalling that the moments are expressed in terms of the continued fraction coefficients,² relations among these coefficients can be obtained. More precisely,

$$\begin{aligned} \mu_i(2p) &= \mu_i(b_p, a_{p-1}, b_{p-1}, \dots, b_1, \epsilon_i), \\ \mu_i(2p+1) &= \mu_i(a_p, b_p, a_{p-1}, b_{p-1}, \dots, b_1, \epsilon_i) \end{aligned} \quad (2.19)$$

and

$$A_q = A_q(\{a_p, b_p\}), \quad p \leq q,$$

$$B_q = B_q(b_q, \{a_p, b_p\}), \quad p \leq q-1. \quad (2.22)$$

Now, proceeding this way, the calculation of the continued fraction coefficients becomes cumbersome and ill conditioned. However, the main point is summarized in the above relations, Eqs. (2.21) and (2.22), which give the number of coefficients a_p and b_p that one must know in order to calculate the coefficients A_q and B_q . Note that these relations are a direct and more precise way of expressing Eq. (2.13).

Let us now summarize the principle of solution of the CPA equations within the present approach. On one hand, we have seen that the effective medium in which an atom is embedded is determined by the self-energy $\sigma(z)$, and the interactor $\Delta(z)$, associated with site n and coupled with the effective medium, which depends on $\sigma(z)$, as indicated in Eq. (2.12). This can be used with a recursion procedure to calculate the coefficients a_p and b_p as functions of the $\{A_q, B_q\}$ according to Eqs. (2.16), or relations I. On the other hand, Eq. (2.13) allows us to relate by a simple moment analysis the A_q and B_q to the $\{a_p, b_p\}$ by Eqs. (2.21) and (2.22), or relations II. Then we use successively the relations II, I, II, I, II, ..., which is another way of expressing the iterative procedure required to achieve self-consistency in the classical solution of the CPA equations. For example, A_0 can be calculated from II, then a_1 and b_1 are calculated from I, then A_1 and B_1 are calculated from II and so on... . Now that we have given the principle of our approach we consider the more technical points. We consider first the calculation of a_p and b_p (relations I), and show by an analysis of a recursion procedure how to obtain the coefficients A_q and B_q that one needs to know at any given step. Then we describe the calculation of A_q and B_q from a_p and b_p (relations II). To this end, we introduce first the concept of sum space, and the calculation of averages of operators in this space. We apply this concept to the treatment of relations II, and show that $\sigma(z)$ is the self-energy associated with an orbital for a Hamiltonian whose matrix elements depend on a_p and b_p . This allows us to calculate A_q and B_q again by a recursion procedure on that Hamiltonian.

C. Extension of the recursion vectors

Starting from an orbital centered on a given site, let us analyze a recursion procedure to determine the coefficients A_q and B_q which are needed to calculate the recursion vector $|p\rangle$ and the coefficients a_p and b_p . The generalization to the multiorbital case is straightforward, and will be discussed later. In the recursion procedure, one calculates the set of recursion vectors $|p\rangle$ according to the following recurrence relation:

$$H|p\rangle = a_p|p\rangle + b_p|p-1\rangle + b_{p+1}|p+1\rangle, \quad (2.23)$$

with $b_0=0$, and the condition that, at each step, the recursion vectors are orthonormal, i.e.,

$$\langle p|q\rangle = \delta_{pq}. \quad (2.24)$$

As is well known, for a TB Hamiltonian, the states $|p\rangle$ extend progressively from the initial orbital centered on a given site, which corresponds to $|0\rangle = |0\rangle$. Thus one needs to know only the matrix elements of the Hamiltonian between orbitals located at different site positions on which $|p\rangle$ has a nonzero component. In Fig. 3, we present the progressive extension of this vector in the case of an alloy based on an infinite linear chain. At each step $|p\rangle \rightarrow |p+1\rangle$, the wave function has components one step further on the semilinear chains. Thus, it is clear that $|p\rangle$ will have nonzero components up to site $(p-1)$ of the semilinear chain attached to the first neighbors and up to site $(p-2)$ for the second neighbors, and so on. If we call neighbor of order q a

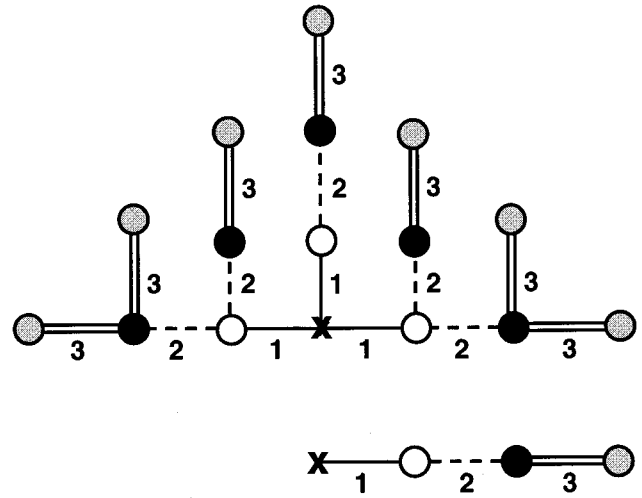


FIG. 3. Equivalent representations of $G_{\text{eff}}(z)$ by a lattice, here an infinite linear chain with each site "dressed" by a semilinear chain representing $\sigma(z)$ (top part), and by a semilinear chain in the recursion basis (bottom part). The extension of the recursion vector, at each step, here 1-3, is represented by solid, dashed, and double solid lines, respectively.

site which can be reached from the site at the origin in q steps, i.e., corresponding to the application of H^q to $|0\rangle$, then we conclude that $|p\rangle$ has nonzero components up to site $(p-q)$ of the semilinear chain attached to a neighboring site of order q . Since a_p and b_{p+1}^2 are calculated from

$$a_p = \langle p|H|p\rangle, \quad p \geq 1,$$

$$b_{p+1}^2 = \|H|p\rangle - a_p|p\rangle - b_p|p-1\rangle\|^2, \quad p \geq 0, \quad (2.25)$$

the values of a_p and b_p can be determined provided we know all the coefficients of the series $A_0, B_1, A_1, B_2, \dots$ up to A_{p-1} and B_{p-1} , respectively. This justifies the formal expression given by Eqs. (2.16).

D. Sum space and its properties

In the study of chemically disordered systems, one has to calculate average values of operators or of some matrix elements of operators. For example, in the calculation of the density of states, we are primarily interested in the diagonal element of the resolvent of the Hamiltonian. We will show that the sum space is a natural and general frame for the calculation of these averages, and that it is related to the augmented space which has been introduced by Mookerjee¹³ to describe specifically substitutional alloys.

1. Operators in the sum space

Let us consider a set of systems $\{S_i\}$ associated with the set of vectors $\{|n\rangle_{S_i}\}$. For simplicity, we consider the case where there is a one to one correspondence between the vectors of the different systems S_i . The Hilbert space for each system S_i is generated by these vectors. Let us define S as the sum space¹⁶ generated by the $|n\rangle_{S_i}$ for all $|n\rangle$ and all S_i . For any operator A_i acting on S_i , the average of the matrix elements of A_i can be written as

$$\bar{A}_{nm} = \sum_i p_i \langle n | A_i | m \rangle_{S_i}, \quad (2.26)$$

where p_i is the probability associated with S_i . From the A_i one can define the sum-operator A in the sum-space S as

$$A = \sum_i \tilde{A}_i, \quad (2.27)$$

where the action of \tilde{A}_i in S is simply given by

$$\tilde{A}_i |n\rangle_{S_j} = A_i |n\rangle_{S_i} \delta_{ij}. \quad (2.28)$$

In other words, \tilde{A}_i is now an operator acting in S , but its action in S_i is the same as for A_i , and for any other S_j , \tilde{A}_i has no action. With this property it is straightforward to establish the relation

$$\bar{A}_{nm} = \sum_i p_i \langle n | A_i | m \rangle_{S_i} = \langle n(p) | A | m(p) \rangle, \quad (2.29)$$

where $|\alpha(p)\rangle = \sum_i \sqrt{p_i} |\alpha\rangle_{S_i}$, and α is equal to n or m . Thus, the average of the matrix elements of A_i is formally related to a matrix element of the sum-operator $A = \sum_i \tilde{A}_i$, with \tilde{A}_i being the extension of A_i in the sum-space $S = \sum_i S_i$. The sum-operator A has some useful properties that we now derive.

2. Properties in the sum space

Let us consider two operators \tilde{A}_i and \tilde{B}_j with the obvious property

$$\tilde{A}_i \tilde{B}_j = \tilde{A}_i \tilde{B}_j \delta_{ij} = \tilde{A}_i \tilde{B}_j \delta_{ij}. \quad (2.30)$$

Then one readily gets

$$A^n = \sum_i (\tilde{A}_i^n) \quad (2.31)$$

for $n \geq 0$. It is also easy to prove that

$$A^{-1} = \sum_i (\tilde{A}_i^{-1}) \quad (2.32)$$

and then finally

$$A^n = \sum_i \tilde{A}_i^n \quad (2.33)$$

for any integer n , positive or negative.

By extension, we expect that a function of an operator, $f(A)$, will be given by

$$f(A) = \sum_i f(\tilde{A}_i). \quad (2.34)$$

We note that for any operator A_i which can be diagonalized, this relation is straightforward in the basis of S that diagonalizes each \tilde{A}_i , and the same will hold for functions of several operators. As an example, consider the Green operator,

$$G(z) = \frac{1}{z-H} = \sum_i \tilde{G}_i(z), \quad (2.35)$$

with $\tilde{G}_i = (z - H_i)^{-1}$, and H_i is the Hamiltonian which describes the system S_i . Then,

$$\sum_i p_i \left\langle \alpha \left| \frac{1}{z-H_i} \right| \alpha \right\rangle_{S_i} = \left\langle \alpha \left| \frac{1}{z-H} \right| \alpha \right\rangle_S, \quad (2.36)$$

where $|\alpha\rangle_S = \sum_i \sqrt{p_i} |\alpha\rangle_{S_i}$. This equality will be used in the next subsection to solve the self-consistent CPA equations, and to give us a relation between $\sigma(z)$ and $\bar{\Delta}_0(z)$.

3. Relation between the sum space and the augmented space

In the case of a substitutional alloy, assumed here for the sake of clarity of exposition to be a binary alloy, each system S_i of the configuration sum space is associated with a given configuration S_i of the alloy. Therefore, a system S_i will be specified by the configuration of each site n ($n=1, N$) of the lattice on which the alloy is based. This configuration is determined by a set of occupation numbers $p_n(i)$, which indicates that site n of S_i is in the configuration S_i . Thus, the set of all states $\{|n\rangle_{S_i}\}$ in the basis is isomorphic to the tensorial product,

$$|n\rangle \times |1, p_1(i)\rangle \times |2, p_2(i)\rangle \times \dots \times |N, p_N(i)\rangle, \quad (2.37)$$

where each p_n takes the value 0 or 1 depending on the occupation of site n by an A or a B species, respectively.

We see that the sum space is isomorphic to a tensorial product of the Hilbert space spanned by the orbitals $\{|n\rangle\}$ with the configuration space which is generated by the vectors

$$|\phi\rangle = |1, p_1(i)\rangle \times |2, p_2(i)\rangle \times \dots \times |N, p_N(i)\rangle. \quad (2.38)$$

If we define Ψ as being the sum space, \mathcal{H} the Hilbert space spanned by the orbitals, and Φ the configuration space, we can write formally

$$\Psi = \mathcal{H} \times \Phi, \quad (2.39)$$

which is the starting relation on which the augmented space formalism derived by Mookerjee is based.¹⁵ Thus, rather than working in the sum space of all alloy configurations, we can equivalently work in the product space as done in Ref. 13. In the framework of the sum space formalism, the average of a matrix element of an operator over all alloy configurations will be written as

$$\overline{\langle n | A_i | m \rangle_{S_i}} = \langle n(\mathcal{P}) | A | m(\mathcal{P}) \rangle, \quad (2.40)$$

where \mathcal{P} is the probability distribution for all the configurations i . If \mathcal{P}_i is the probability of configuration i , then

$$\mathcal{P}_i = \mathcal{Q}_1(p_1(i)) \mathcal{Q}_2(p_2(i)) \dots \mathcal{Q}_N(p_N(i)), \quad (2.41)$$

where \mathcal{Q}_n is the probability distribution for all the accessible configurations at site n .

In the case of a periodic lattice with one atom per unit cell, \mathcal{Q}_n does not depend on n . In Eq. (2.40), $\alpha(\mathcal{P})$ (where $\alpha = n, m$) is defined as

$$|\alpha(\mathcal{P})\rangle = \sum_i \sqrt{\mathcal{P}_i} |\alpha\rangle_{S_i} = |n\rangle |\alpha_1\rangle \cdots |\alpha_N\rangle, \quad (2.42)$$

where

$$|\alpha_n\rangle = \sum_{p=0,1} \sqrt{Q_n(p)} |n, p_n\rangle \quad (2.43)$$

since for a binary alloy p can only take two values, 0 or 1, on every site. Hence, we recover the formulation of averages in the augmented space formalism. This formalism has been proven useful for the study of substitutional alloys,^{14,17-19} and this suggests that the sum-space formalism can be equally useful. However one can work along a different path within the sum-space representation. For example, the above change in the basis which leads to the product space illustrates this. We will show below that a change in the basis also allows us to derive a number of useful relations.

E. Calculation of the coefficients of continued fraction

We have seen from the analysis of the moments $\mu(p)$, in Sec. II B, that the coefficients A_q and B_q can be calculated step by step from the coefficients (a_p, b_p) . In this subsection, we use the properties of the sum space to derive a formal relation between σ and Δ . First, we consider the case of a binary alloy. Note that the derivation given in Ref. 20 for binary alloys is difficult to extend to the case of higher-order multicomponent alloys, whereas the sum-space formalism leads to a straightforward generalization as will be shown for the case of ternary and quaternary alloys.

1. Binary alloys

For binary alloys, the self-consistency condition within the CPA reads:

$$\sum_{i=A,B} c_i G_i(z) = G(z), \quad (2.44)$$

with

$$G_i(z) = [z - \epsilon_i - \Delta(z)]^{-1},$$

$$G(z) = [z - \sigma(z) - \Delta(z)]^{-1}. \quad (2.45)$$

Using the representation of σ and Δ in terms of semi-infinite linear chains, G_i and G can be viewed as the diagonal elements of Green operators on site $|0\rangle_i$ and $|0\rangle$, respectively, of the systems S_i and S which are represented in Fig. 4. Using Eq. (2.36) derived in Sec. II D 2, we get

$$\sum_{i=A,B} c_i G_i(z) = \left\langle 0 \left| \frac{1}{z - H} \right| 0 \right\rangle, \quad (2.46)$$

where H is the sum Hamiltonian associated with systems S_A and S_B , i.e., $H = \tilde{H}_A + \tilde{H}_B$. In other words, H is the Hamiltonian of the global system S made of the two uncoupled systems S_A and S_B , each associated with its Hamiltonian \tilde{H}_A and \tilde{H}_B , respectively.

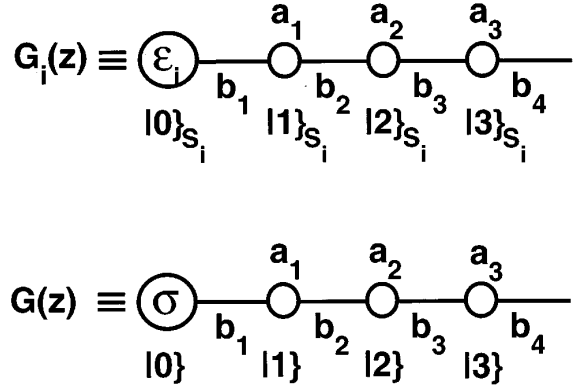


FIG. 4. Schematic representation of $G_i(z)$ and $G(z)$ associated with \tilde{H}_i and H , respectively, in the original basis.

The sum Hamiltonian can now be conveniently expressed in a new basis, different from the original basis $\{|p\rangle_{S_A}, |p\rangle_{S_B}; p=0,1,2, \dots\}$. For each p , we define two orthonormal states

$$|p\rangle_S = \sqrt{c_A} |p\rangle_{S_A} + \sqrt{c_B} |p\rangle_{S_B},$$

$$|p\rangle_{AS} = \sqrt{c_B} |p\rangle_{S_A} - \sqrt{c_A} |p\rangle_{S_B}, \quad (2.47)$$

which generate the sum-space $S = S_A \oplus S_B$. One has obviously the relations

$${}_S\langle p|q\rangle_S = \delta_{pq},$$

$${}_{AS}\langle p|q\rangle_{AS} = \delta_{pq},$$

$${}_{AS}\langle p|q\rangle_S = {}_S\langle q|p\rangle_{AS} = 0. \quad (2.48)$$

It is then easy to express any matrix element of H in this new orthonormal basis. Since all matrix elements of \tilde{H}_A and \tilde{H}_B are identical except for the on-site terms associated with $|0\rangle_A$ and $|0\rangle_B$, one gets for $(p, q) \neq (0, 0)$

$${}_S\langle p|H|q\rangle_S = {}_{AS}\langle p|H|q\rangle_{AS} = {}_{S_A}\langle p|\tilde{H}_A|q\rangle_{S_A} = {}_{S_B}\langle p|\tilde{H}_B|q\rangle_{S_B},$$

$${}_S\langle p|H|q\rangle_{AS} = {}_{AS}\langle q|H|p\rangle_S = 0, \quad (2.49)$$

and for $(p, q) = (0, 0)$,

$${}_S\langle 0|H|0\rangle_S = c_A \epsilon_A + c_B \epsilon_B \equiv \epsilon_S,$$

$${}_{AS}\langle 0|H|0\rangle_{AS} = c_B \epsilon_A + c_A \epsilon_B \equiv \epsilon_{AS},$$

$${}_S\langle 0|H|0\rangle_{AS} = {}_{AS}\langle 0|H|0\rangle_S = \sqrt{c_A c_B} (\epsilon_A - \epsilon_B) \equiv U. \quad (2.50)$$

The Hamiltonian H expressed in this new basis is schematically represented in Fig. 5. The formal expression for the average of the Green functions $G_A(z)$ and $G_B(z)$ implies that $c_A G_A(z) + c_B G_B(z)$ is the Green function on the site occupied by the vector $|0\rangle_S$ for the Hamiltonian represented in Fig. 4. Therefore, the self-consistency condition imposes the equality of the diagonal elements of Green functions on the first site of the semilinear chain associated with the vector $|0\rangle_S$ of Fig. 5 (top), and on the first site of the semilinear chain associated with $|0\rangle$ of Fig. 4 or equivalently, of Fig. 5

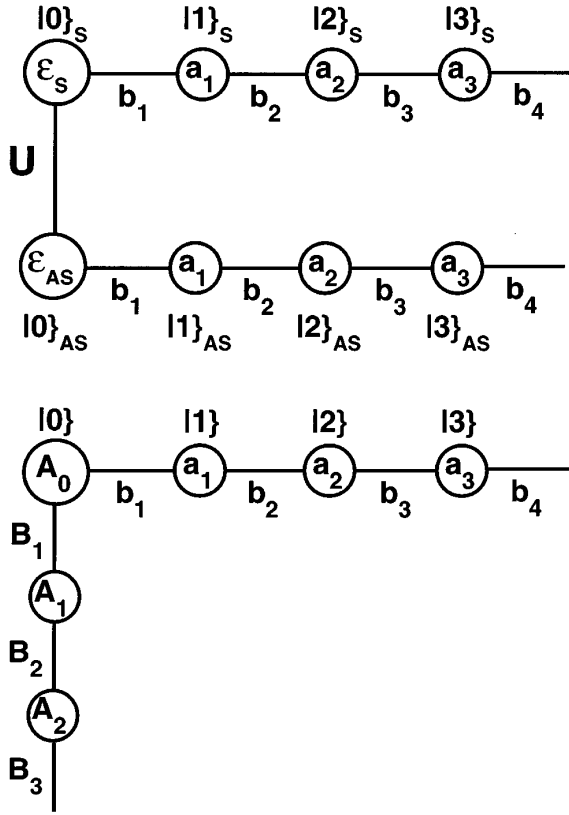


FIG. 5. Schematic representation of the Hamiltonian H expressed in the new basis $\{|p\rangle_S, |p\rangle_{AS}\}$ (top), and compared with its representation in the original basis $\{|p\rangle\}$ (bottom) for a binary alloy.

(bottom). Consequently the self-energy $\sigma(z)$ is represented by the coupling to the semi-infinite linear chain of Fig. 5 (bottom), and by simple identification, this function is analytically given by

$$\sigma(z) = \epsilon_S + \frac{U^2}{z - \epsilon_{AS} - \Delta(z)}, \quad (2.51)$$

which, with an appropriate change in the notations, is identical to expression (17) given in Ref. 20.

By identification of the continued fraction expansions of $\sigma(z)$ and $\Delta(z)$, we then obtain

$$\begin{aligned} A_0 &= \epsilon_S, \\ A_1 &= \epsilon_{AS}, \\ B_1^2 &= U^2, \\ &\dots \\ B_q &= b_{q-1}, \quad q \geq 2, \\ A_q &= a_{q-1}, \quad q \geq 2. \end{aligned} \quad (2.52)$$

2. Ternary and higher-order multicomponent alloys

For an alloy containing n_c components, Eq. (2.36) can be rewritten as

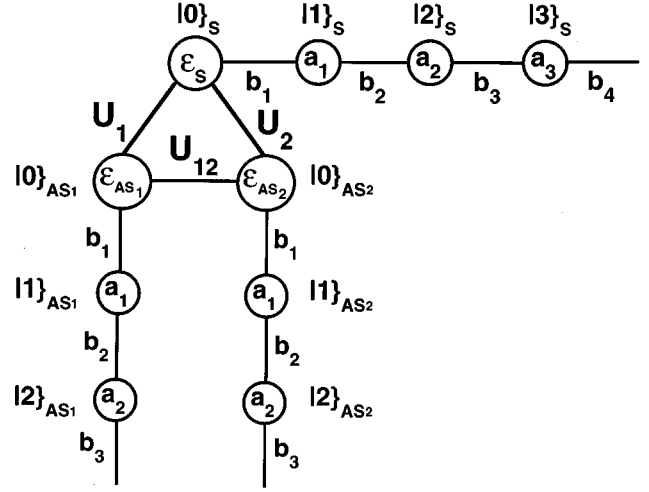


FIG. 6. Schematic representation of the Hamiltonian H expressed in the new basis $\{|p\rangle_S, |p\rangle_{AS_1}, |p\rangle_{AS_2}\}$ for a ternary alloy.

$$\sum_{i=1, n_c} c_i G_i(z) = \left\langle 0 \left| \frac{1}{z - H} \right| 0 \right\rangle, \quad (2.53)$$

where $|0\rangle = \sum_{i=1, n_c} \sqrt{c_i} |0\rangle_{S_i}$ and $H = \sum_{i=1, n_c} \tilde{H}_i$, with \tilde{H}_i being the Hamiltonian associated with the semilinear chain representing the continued fraction expansion of G_i . Again, the initial basis $\{|p\rangle_{S_i}\}$ is replaced by

$$|p\rangle_S = \sum_{i=1, n_c} \sqrt{c_i} |p\rangle_{S_i},$$

$$|p\rangle_{AS_j} = \sum_{i=1, n_c} u_{ji} |p\rangle_{S_i}, \quad j = 1, n_c - 1. \quad (2.54)$$

The choice for the coefficients u_{ji} is such that the new basis must be orthonormal. However, we note that this choice is not unique since the space orthogonal to $|p\rangle_S$ is of dimension $n_c - 1$, for a given p . Since the \tilde{H}_i only differ by the on-site energies associated with $|0\rangle_{S_i}$, one gets for $(p, q) \neq (0, 0)$,

$$\begin{aligned} {}_S \langle p | H | q \rangle_S &= {}_{AS_j} \langle p | H | q \rangle_{AS_j}, \quad j = 1, n_c - 1, \\ &= {}_{S_i} \langle p | \tilde{H}_i | q \rangle_{S_i}, \quad i = 1, n_c, \end{aligned} \quad (2.55)$$

and for $(p, q) = (0, 0)$,

$${}_S \langle 0 | H | 0 \rangle_S = \sum_{i=1, n_c} c_i \epsilon_i \equiv \epsilon_S, \quad (2.56)$$

with the other matrix elements of H easily determined once the particular choice for $\{u_{ji}\}$ is made. Let us define

$$\begin{aligned} \epsilon_{AS_i} &= {}_{AS_i} \langle 0 | H | 0 \rangle_{AS_i}, \quad i = 1, n_c - 1, \\ U_i &= {}_S \langle 0 | H | 0 \rangle_{AS_i}, \quad i = 1, n_c - 1, \\ U_{ij} &= {}_{AS_i} \langle 0 | H | 0 \rangle_{AS_j}, \quad i, j = 1, n_c - 1, \end{aligned} \quad (2.57)$$

with $U_{ij} = U_{ji}$.

Then the Hamiltonian H expressed in the new basis is schematically represented in Fig. 6. The expression (2.53)

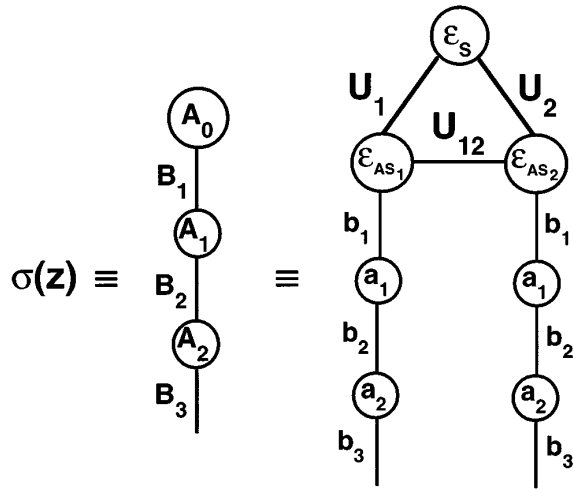


FIG. 7. Equivalent representations of the self-energy $\sigma(z)$ in the case of a ternary alloy.

shows that $\sum_i c_i G_i(z)$ is given by the diagonal element of $\{0|(z-H)^{-1}|0\}$ in the sum space. Therefore, $\sigma(z)$ is simply obtained by identification of the representations of $G(z)$ in the old and the new basis, given in Fig. 5 (bottom) and Fig. 6, respectively. Contrary to the binary case, this time we do not have an analytic expression for $\sigma(z)$ as a function of $\Delta(z)$. Note, however, that since we are interested in the determination of the coefficients (A_q, B_q) of the continued fraction expansion for $\sigma(z)$, we can simply calculate them for the system represented in Fig. 7 (right-side representation) by an additional recursion scheme. With an analysis similar to that given in Sec. IIC regarding the extension of the recursion vectors, we conclude that

$$A_q = A_q(a_{q-1}, b_{q-1}, a_{q-2}, b_{q-2}, \dots, b_1), \quad q \geq 2,$$

$$B_q = B_q(b_{q-1}, a_{q-2}, b_{q-2}, \dots, b_1), \quad q \geq 2, \quad (2.58)$$

and A_0 is immediately given by $A_0 = \sum_{i=1, n_c} c_i \epsilon_i$. We also note that B_1 and A_1 do not depend on $\Delta(z)$ via its coefficients (a_p, b_p) since the vector $|1\rangle$ has a nonzero projection only on $|0\rangle_S$ and $|0\rangle_{AS_j}$ ($j=1, n_c-1$). As a further example of the extension to higher-order multicomponent alloys, we give in Fig. 8, the equivalent representations of the self-energy $\sigma(z)$ in the case of a quaternary alloy.

F. Summary of the methodology and extension to the multiorbital case

The principle of our approach is to deal with the equations of the CPA theory within the locator formalism. The two functions which naturally appear in this formalism are $\sigma(z)$, which is the self-energy associated with an orbital and which represents the effect of chemical disorder, and $\Delta(z)$, the so-called renormalized interactor, which refers to the coupling of an orbital centered on a given site with the effective CPA medium.

First, within the CPA theory, the Herglotz property of these two functions allows us to consider their continued fraction representations. Hence, the determination of $\sigma(z)$

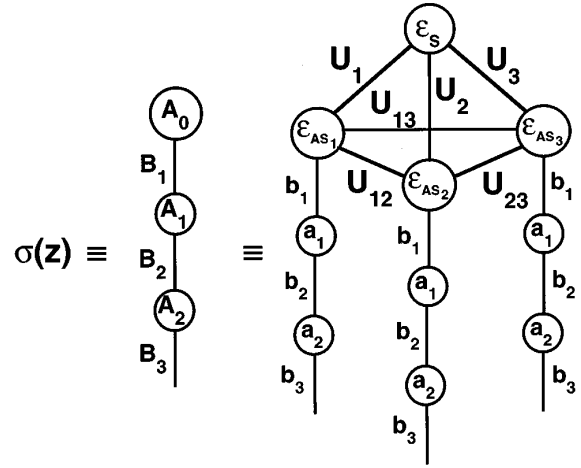


FIG. 8. Equivalent representations of the self-energy $\sigma(z)$ in the case of a quaternary alloy.

and $\Delta(z)$ at all complex energies z becomes possible through the calculation of the coefficients of their continued fraction expansions.

Second, we use the well-known equivalence between a continued fraction expansion and its representation in terms of a semilinear chain, in which case the matrix elements of the Hamiltonian associated with this chain are the coefficients of the continued fraction. Replacing $\sigma(z)$ by the coupling to a semilinear chain leads to the definition of an energy-independent effective Hamiltonian. The calculation of average Green operator matrix elements can then be performed by real-space methods such as the recursion, and properties derived from the electronic structure, such as density of states, integrals over the density of states (e.g., energetics, effective interactions), or transport properties can be predicted in a very efficient way. Third, in order to solve the self-consistent CPA equations, we use alternatively two relations, namely, $\Delta(z)$, which depends on the effective environment, and is a function of $\sigma(z)$, and $\sigma(z)$, by the CPA self-consistency condition, which is a function of $\Delta(z)$.

By performing a recursion with a starting vector being one of the atomic orbitals centered on a given site, we can make use of the first relation: $\Delta(z) = f[\sigma(z)]$, with the introduction of an energy-independent effective Hamiltonian. We calculate the a_p and b_p :

$$a_p = a_p(A_{p-1}, B_{p-1}, \dots, A_1, B_1, A_0),$$

$$b_p = b_p(B_{p-1}, A_{p-1}, \dots, A_1, B_1, A_0). \quad (2.59)$$

If there are several inequivalent orbitals, $\lambda = 1, n_o$, then one must consider a set of renormalized interactors $\Delta_\lambda(z)$ and self-energies $\sigma_\lambda(z)$ associated with each of these orbitals. Then the coefficients a_p^λ and b_p^λ , expressed as

$$a_p^\lambda = a_p^\lambda(A_{p-1}^\mu, B_{p-1}^\mu, \dots, A_1^\mu, B_1^\mu, A_0^\mu),$$

$$b_p^\lambda = b_p^\lambda(B_{p-1}^\mu, A_{p-1}^\mu, \dots, A_1^\mu, B_1^\mu, A_0^\mu), \quad (2.60)$$

are calculated with a recursion procedure by starting from each of the n_o inequivalent orbitals, i.e., by performing n_o recursions in parallel. Note that this procedure becomes well-suited for a practical implementation on a parallel computer.

Then, we can explore the CPA self-consistency condition, i.e., the second relation which relates $\sigma(z)$ to $\Delta(z)$. In the multiorbital case, one gets a set of self-consistency conditions, $\sigma_\lambda(z) = g[\Delta_\lambda(z)]$. Note that these equations do not couple different λ 's in contrast to the previous set of relations $\Delta_\lambda(z) = f[\sigma_\mu(z)]$ which does. Again by an application of the recursion scheme, we get

$$\begin{aligned} A_q^\lambda &= A_q^\lambda(a_{q-1}^\lambda, b_{q-1}^\lambda, \dots, b_1^\mu), \\ B_q^\lambda &= B_q^\lambda(b_{q-1}^\lambda, a_{q-2}^\lambda, \dots, b_1^\mu). \end{aligned} \quad (2.61)$$

The final solution of the CPA problem is obtained by using alternatively the two sets of relations mentioned above. In addition to the real-space aspect of the solution, this new methodology can be easily extended to account for off-diagonal disorder within the Shiba approximation¹⁵ or the approach of Blackman, Esterling, and Berk,^{21,22} as will be shown in a forthcoming publication, and can be applied to other approximations such as the cluster Bethe lattice method,²³ or the calculation of transport properties in disordered alloys.

III. EMBEDDED CLUSTER METHOD AND THE ORBITAL-PEELING TECHNIQUE

Since the ECM has been compared in detail with other approaches which are also based on the electronic structure of the chemically disordered state of an alloy,¹⁰ we only present the main results here.

A. Embedded cluster method

Let us consider a system consisting of a cluster \mathcal{C}_{n_k} of n_k sites, embedded in a disordered material. An exact treatment of this system would require a complete configurational average over all configurations of the material surrounding the cluster. Clearly, approximations must be made to solve the problem. At the first level of approximation, all sites outside the cluster are taken as being occupied by effective medium scatterers, or ‘‘CPA atoms.’’ The configurational (or ordering) energy is then given by

$$\begin{aligned} E(\{\delta c_n\}, E_F) &= E_{\text{CPA}} + \sum_n V_n^{(1)} \delta c_n + \frac{1}{2} \sum_{m,n} V_{nm}^{(2)} \delta c_n \delta c_m \\ &+ \frac{1}{3} \sum_{l,m,n} V_{lmn}^{(3)} \delta c_l \delta c_m \delta c_n + \dots, \end{aligned} \quad (3.1)$$

where δc_n refers to the fluctuation of local concentration, as discussed in the Introduction. In this equation, E_{CPA} is the energy associated with the CPA medium, and $V_{n_1, n_2, \dots, n_k}^{(k)}$ is an effective cluster interaction defined within the ECM as

$$V_{n_1 n_2 \dots n_k}^{(k)} = [V_{n_1 n_2 \dots n_{k-1} n_k}^{(k-1)}]_{n_k}^A - [V_{n_1 n_2 \dots n_{k-1} n_k}^{(k-1)}]_{n_k}^B. \quad (3.2)$$

The double primes in Eq. (3.1) denote that the sums are performed over distinct sets of sites, i.e., all the n_i indices are different, as opposed to the GPM expansion where the restrictions apply to consecutive sites only, and lead to self-

retracing scattering contributions to the effective pair interactions (EPI's) such as $V_{mmmn}^{(4)}$, $V_{mmmmn}^{(6)}$,

The symbol $[V_{n_1 n_2 \dots n_{k-1} n_k}^{(k-1)}]_{n_k}^i$ in Eq. (3.2) denotes an effective multisite interaction among the n_k sites of cluster \mathcal{C}_{n_k} , under the restriction that site n_k is occupied by an atom of type i . It has been shown that the ECM and the GPM are closely related,¹⁰ with the former corresponding to a summation of a set of diagrams (terms) of the latter. Note that, as in any perturbation theory which relies on the CPA medium, the small parameter in the GPM only depends on the scattering properties of the electrons, which means that the expansion for the ordering energy is valid even for large fluctuations of local concentrations. In practice, the second order contribution to the EPI, $V_{nm}^{(2)}$, within the GPM is essentially numerically indistinguishable from the full summation provided by the ECM of all scattering processes taking place between the two sites n and m . One advantage of the ECM is that it allows the calculation of local densities of states within a cluster, with a specific atomic configuration, embedded in the CPA medium, and thus the study of local environment effects on the electronic structure properties of alloys.

B. Calculation of the effective interactions and the orbital-peeling method

The energy $V_n^{(1)}$ in Eq. (3.1) is an effective single-site interaction which, by definition, is associated with the interchange of a B species with an A species at site n . This interaction is simply given by

$$V_n^{(1)} = \int_{-\infty}^{E_F} (\epsilon - E_F) (n_n^B(\epsilon) - n_n^A(\epsilon)) d\epsilon, \quad (3.3)$$

where E_F is the Fermi energy of the CPA medium, and

$$n_n^i(\epsilon) = -\frac{\text{Im}}{\pi} \lim_{\eta \rightarrow 0^+} G_{nn}^{ii}(\epsilon + i\eta), \quad (3.4)$$

with i referring to the species, and

$$G_{nn}^{ii}(z) = [z - \epsilon_n^i - \Delta_n(z)]^{-1}. \quad (3.5)$$

Note that for alloys based on a periodic lattice with one site per cell, the total single-site contribution to the configurational energy is zero since $V_n^{(1)}$ does not depend on the site index n , and $\sum_{n=1}^N \delta c_n = 0$, where N is the number of sites in the crystal.

The effective two-site (or pair) interaction (or EPI), $V_{nm}^{(2)}$, is given by the difference in single-site interactions at site n when site $m \neq n$ is occupied by an A or a B species. This energy difference is by definition given by

$$V_{nm}^{(2)} = \int_{-\infty}^{E_F} (\epsilon - E_F) \Delta n_{nm}(\epsilon) d\epsilon, \quad (3.6)$$

where

$$\Delta n_{nm}(\epsilon) = -\frac{2}{\pi} \text{Im} \lim_{\eta \rightarrow 0^+} \sum_{ij} s_{ij} \langle \text{Tr}(zI - H_{nm}^{ij})^{-1} \rangle, \quad (3.7)$$

with $s_{ij} = +1$ or -1 depending on whether or not $i = j$, and the sum extending over all possible combinations of pairs ij ($i, j = A, B$ for the case of a binary alloy). The operator H_{nm}^{ij} is the Hamiltonian of a system where all sites except n and m are occupied by species i and j , respectively. The factor 2 in Eq. (3.7) accounts for the spin degeneracy, and the trace, Tr , refers to a sum over the n_o orbitals. The symbol $\langle \rangle$ denotes a configurational averaging over all sites except n and m . This EPI can be expressed in terms of the phase shift $\eta(z)$ according to

$$V_{nm}^{(2)} = -\frac{2}{\pi} \int_{-\infty}^{E_F} d\epsilon (\epsilon - E_F) \frac{d\eta_{nm}(z)}{dz}, \quad (3.8)$$

where

$$\eta_{nm}(z) = \ln \frac{\det \langle G_{nm}^{AA} \rangle \det \langle G_{nm}^{BB} \rangle}{\det \langle G_{nm}^{AB} \rangle \det \langle G_{nm}^{BA} \rangle}, \quad (3.9)$$

with G_{nm}^{ij} being the resolvent of the Hamiltonian H_{nm}^{ij} .

In a conventional calculation, for a binary alloy characterized by n_o orbitals, the determination of one EPI involves, without reference to any symmetry of the lattice, $2^2 n_o^2$ calculations. It was shown in the mid 70's by Burke¹² that such a determination can be achieved with only $2^2 n_o$ calculations with the so-called orbital-peeling method (OPM). This method also offers the advantage that only site-diagonal elements of Green functions (and not the off-diagonal ones) need to be calculated. Within the OPM, the expression (3.6) for the EPI is rewritten as

$$V_{nm}^{(2)} = -\frac{2}{\pi} \text{Im} \sum_{ij} s_{ij} \sum_{\lambda=1}^{n_o} \delta X, \quad (3.10)$$

where

$$\begin{aligned} \delta X &= \int_{-\infty}^{E_F} (\epsilon - E_F) \ln \langle G_{nm}^{\lambda,ij} \rangle d\epsilon \\ &= \sum_{\alpha=1}^{p-1} z_{\alpha}^{\lambda,ij} - \sum_{\alpha=1}^p p_{\alpha}^{\lambda,ij} + (n_p^{\lambda,ij} - n_Z^{\lambda,ij}) E_F. \end{aligned} \quad (3.11)$$

In this last expression, $G_{nm}^{\lambda,ij}$ is the resolvent of a Hamiltonian $H_{nm}^{\lambda,ij}$ which defines a system where the two species i and j located at sites n and m , respectively, are embedded in the average medium (here, the CPA medium), and for which the orbitals from 1 to $\lambda - 1$ are omitted at site n . The quantities $z_{\alpha}^{\lambda,ij}$ and $p_{\alpha}^{\lambda,ij}$ are the zeros and the poles of $G_{nm}^{\lambda,ij}$, up to the Fermi energy, which is indicated by the summation over α up to $p - 1$ in the case of the zeros, and up to p in the case of the poles. The $n_Z^{\lambda,ij}$ and $n_p^{\lambda,ij}$ correspond to the numbers of zeros and poles, respectively.

With this OPM, one avoids the numerical integration of Eq. (3.6). In addition, the zeros and the poles of the Green function $G_{nm}^{\lambda,ij}$ are easily determined in the context of the CPA-extended recursion presented above. Indeed, the poles correspond to the eigenvalues of a tridiagonal matrix \mathcal{P} whose elements are $\mathcal{P}_{nn} = a_n$ and $\mathcal{P}_{n,n-1} = \mathcal{P}_{n-1,n} = b_{n-1}$, and the zeros are given by the eigenvalues of a tridiagonal matrix \mathcal{Z} obtained from the matrix \mathcal{P} by deleting its first column and row. This eigenvalue problem is well conditioned, and a

great accuracy can be achieved in the determination of the zeros and the poles entering expression (3.11).

To ensure a continuous variation of the EPI's with the Fermi energy (and therefore the band filling), we adopted a slightly modified procedure than the one indicated in Ref. 12. To position a pole of $G_{nm}^{\lambda,ij}$ at the Fermi energy E_F , the last coefficient a_p of the continued fraction expansion is modified. This method preserves all other coefficients of the continued fraction, and thus all the moments of the density of states, except the last one, μ_{2p+1} . Having a pole at E_F implies that the last coefficient a_p^* is given by

$$a_p^* = E_F + \frac{b_{p-1}^2}{a_{p-1} - E_F - \frac{b_{p-2}^2}{a_{p-2} - E_F - \dots - \frac{-b_1^2}{a_1 - E_F}}}. \quad (3.12)$$

With this last modified coefficient, we recompute the poles and the zeros of the Green function and their numbers. Note that this operation can be applied after having extended the continued fraction expansion with a number of a_{∞} and b_{∞}^2 which correspond to the asymptotic values of a_p and b_p^2 , respectively. The asymptotic values of these coefficients, related to the center of the spectral support, a_{∞} , and to its width, $4b_{\infty}$, can be accurately determined in the case of a connected electronic spectrum, i.e., in the absence of a gap, with the Beer-Pettifor method,²⁴ or with the method proposed in Ref. 4 when gaps exist.

In practice, since the self-energy $\sigma_{n\lambda}(z)$ is known by its continued fraction expansion, it is a simple matter to determine the continued fraction expansion of $G_{nm}^{\lambda,ij}$ with a recursion scheme by (i) branching on each site of the real lattice, except at site n and m , a semilinear chain representing $\sigma_n(z)$, or n_o chains representing $\sigma_{n\mu}(z)$, in the multiorbital case; (ii) locating the species i and j at sites n and m , respectively; and (iii) setting the projection of the recursion vector on site n , at each step of the recursion, to zero for the orbitals 1 to $\lambda - 1$, in accordance with the OPM.

IV. APPLICATIONS

To demonstrate the validity and the accuracy of the real-space methodology presented in the previous sections, a number of numerical tests were carried out for bcc-based binary Zr-Rh and ternary Zr-Ru-Rh alloys. These alloys belong to a class of materials which exhibit interesting properties for biocompatible implant device applications.²⁵ To describe their electronic structure properties, the Slater-Koster (SK) parameters which enter the TB Hamiltonian have been extracted from TB LMTO calculations as described in Ref. 25.

The hopping integrals are written in terms of the SK parameters which depend on the occupation of sites n and m by i and j species, respectively, and on the distance r_{nm} between the two sites, as follows:

$$\beta_{ni,mj}^{\lambda,\mu} = \sum_h c_{nm}^h w_{ij}^h(r_{nm}), \quad (4.1)$$

TABLE I. Tight-binding parameters A_{Rh}^h and P_{Rh}^h , see Eq. (4.2), which define the hopping integrals for Rh.

h	A_{Rh}^h (Ry)	P_{Rh}^h (a.u. ⁻¹)
$ss\sigma$	-16.7886	1.0573
$pp\sigma$	13.2390	0.9274
$pp\pi$	-161.7200	1.8024
$dd\sigma$	-8.9922	0.9389
$dd\pi$	158.6201	1.6576
$dd\delta$	-216.2461	2.1738
$sp\sigma$	13.9556	0.9797
$sd\sigma$	-8.8131	0.9439
$pd\sigma$	-9.1538	0.9035
$pd\pi$	187.4781	1.7605

where the $w_{ij}^h(r_{nm})$ refer to the SK parameters, and the c_{nm}^h depend on the direction cosines of vector \mathbf{r}_{nm} . The superscript h runs over the ten SK parameters for spd electronic systems, i.e., $h = ss\sigma, pp\sigma, \dots, dd\sigma, dd\pi, dd\delta, \dots$.²⁶

As in Ref. 25, the SK parameters for the pure metals are assumed to vary with the interatomic distance d , according to

$$w_{ii}^h = A_i^h \exp^{-P_i^h d}, \quad (4.2)$$

where the parameters A_i^h and P_i^h have been fitted to TB-LMTO results obtained for the three alloy components Zr, Ru, and Rh. In the following we will assume a cutoff distance not exceeding the second-neighbor distance in the bcc lattice. These parameters are given in Table I for Rh, and in Table I of Ref. 25 for Zr and Ru. For a particular alloy, the SK parameters have been approximated according to

$$w_{\text{alloy}}^h = \left(\sum_i c_i \sqrt{w_{ii}^h} \right)^2, \quad (4.3)$$

where the w_{ii}^h parameters of the pure species i are calculated at the interatomic distance of the alloy. The equilibrium lattice constants of bcc-based Zr, Ru, and Rh, take the values 6.712 67 a.u., 5.801 941 a.u., and 5.796 79 a.u., respectively, as obtained from scalar relativistic LMTO calculations in the atomic sphere approximation (ASA). These values define the lattice constant of the alloy at any composition by assuming that the atomic volume of the alloy is given by the concentration weighted average of the atomic volumes of the pure species (also known as the Zen's law).

Similarly, a variation of the on-site energies with the lattice parameter a is assumed, and given by a second order polynomial

$$\epsilon_{i\lambda}^0 = A_i^\lambda + B_i^\lambda a + C_i^\lambda a^2, \quad (4.4)$$

where λ refers to s , p , t_{2g} , or e_g . These parameters obtained from a fit to TB-LMTO calculations are given in Table II for Rh, and in Table II of Ref. 25 for Zr and Ru. In the alloy case, the on-site energies of each alloy component are calculated at the lattice constant of the alloy (as described above). To ensure local charge neutrality in a broad range of alloy composition, global shifts δ_i were applied to these on-site energies,

TABLE II. Coefficients A_{Rh}^λ , B_{Rh}^λ , and C_{Rh}^λ , see Eq. (4.4), which define the on-site energies for Rh.

λ	A_{Rh}^λ (Ry)	B_{Rh}^λ (Ry a.u. ⁻¹)	C_{Rh}^λ (Ry a.u. ⁻²)
s	9.407978	-2.689624	0.188783
p	9.613148	-2.606757	0.177081
t_{2g}	6.635920	-1.989722	0.141352
e_g	6.170196	-1.864335	0.132686

$$\epsilon_{i\lambda} = \epsilon_{i\lambda}^0 + \delta_i. \quad (4.5)$$

In the present case, $\delta_{\text{Zr}} = 0$ Ry, $\delta_{\text{Ru}} = 0.358$ Ry, and $\delta_{\text{Rh}} = 0.313$ Ry. With these assumptions, the TB Hamiltonian given in Eq. (1.1) is fully defined, and applications of the methodology described in the previous sections to the study of the electronic structure properties, and of the energetics of binary and higher-order multicomponent alloys can now be presented.

A. Density of states of binary, pseudobinary, and ternary alloys

The electronic densities of states (DOS) were computed with the CPA-extended recursion and compared with the results of the standard k space approach.²⁵ In the latter case, the average Green function was obtained after integration in reciprocal space over the first Brillouin zone with 240 special k points.²⁷ Figure 9 shows the DOS of bcc-based $\text{Zr}_{0.5}\text{Rh}_{0.5}$ obtained with both approaches. In that particular case, the self-energies, each associated with an orbital symmetry (i.e., s , p , t_{2g} , or e_g), were accurately determined with 17 levels of continued fraction, and asymptotic values of the coefficients determined with the Beer-Pettifor method.²⁴ The two DOS are almost indistinguishable.

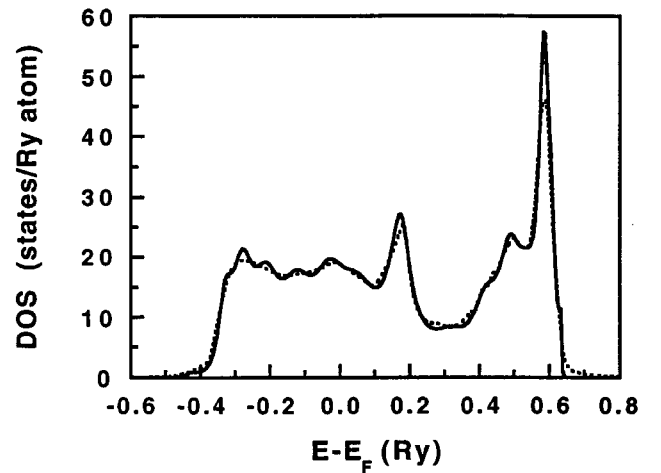


FIG. 9. Density of states of bcc-based $\text{Zr}_{0.5}\text{Rh}_{0.5}$ disordered alloy as a function of energy (the Fermi energy E_F is taken as zero of energy), as obtained from (a) real-space calculations (solid line), and (b) k -space calculations (dotted line), within the CPA. In (a) 17 levels of continued fraction were computed (both on the real crystal and on the semilinear chains associated with each site), and in (b) integration has been performed with 240 special k points.

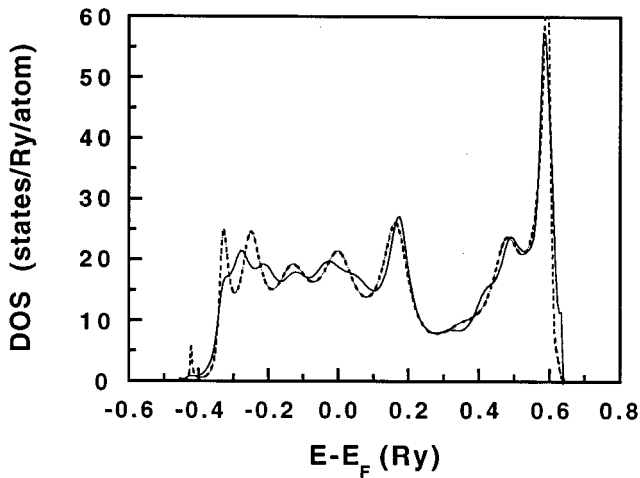


FIG. 10. Density of states of bcc-based $Zr_{0.5}Rh_{0.5}$ disordered alloy as a function of energy (the Fermi energy E_F is taken as zero of energy), as obtained from real-space calculations with: (i) 17 levels of continued fraction on both the real crystal and the semilinear chain (solid line), and (ii) three levels of continued fraction on the real crystal and ten levels along the semilinear chains.

Interestingly enough, the calculation in real space can be performed with an equivalent level of accuracy but with a significant reduction in computational cost (memory allocation and execution time) if the cluster of atoms, which is generated during the recursion procedure is truncated to a size associated with q levels of continued fraction, whereas the semilinear chains are extended up to p ($> q$) levels of continued fraction. In Fig. 10 the DOS of bcc-based $Zr_{0.5}Rh_{0.5}$ obtained with $q=3$ and $p=10$ is almost identical to the one displayed in Fig. 9 with $p=q=17$. In the former case, only 175 sites belonging to the bcc lattice have been generated, as opposed to the 21 455 sites in the latter case. This interesting property, although it depends on the lattice and on the range of the SK parameters, comes about because of the information carried out by the coefficients of continued fraction along the semilinear chain which “dresses,” for each orbital, each site of the lattice.

Since the CPA equations are solved in real space, the electronic structure properties of pseudobinary alloys can be easily studied with minor effort in the practical implementation of the formalism. Suppose that Zr fully occupies one of the simple cubic (sc) sublattice, whereas chemical disorder takes place between Ru and Rh species on the other sublattice. Only the sites of this latter sublattice will be “dressed” with semilinear chains (one per orbital) which represent the self-energies (one per orbital), and the CPA equations for this pseudobinary alloy can be solved in the same way they are for the binary case. For comparison, a similar calculation can be performed with a k -space approach,²⁵ but now the integration has to be done in the Brillouin zone of the simple cubic lattice (in the present case, 816 special k points²⁷ have been used). From Fig. 11 we conclude that the DOS of the pseudobinary $Zr_{0.50}(Ru_{0.25}Rh_{0.25})$ disordered alloy, as obtained by both approaches, compare once again favorably. A similar agreement is achieved in the case of ternary alloys, and an example is given in Fig. 12 for the case of bcc-based

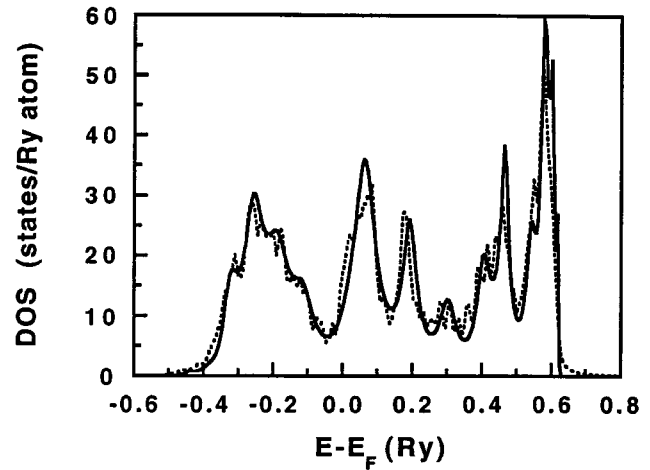


FIG. 11. Density of states of a bcc-based pseudobinary $Zr_{0.50}(Ru_{0.25}Rh_{0.25})$ disordered alloy as a function of energy (the Fermi energy E_F is taken as zero of energy). In the real-space approach (solid line), only the sites of one of the simple cubic sublattices, which are occupied by Ru and Rh atoms, are “dressed” with semilinear chains representing the self-energies, within the CPA, and 17 levels of continued fraction on both the real crystal and the semilinear chain have been determined. In the k -space approach (dotted line), 816 special k points in the irreducible Brillouin zone of the simple cubic lattice have been used for the integration.

$Zr_{0.50}Ru_{0.25}Rh_{0.25}$, for which the CPA was applied to the chemically random ternary system.

It should be reemphasized that, within the real-space methodology, all Green functions, partial per site or per orbital and total, are expressed in terms of continued fractions, whereas, in the k -space approach, they are given numerically. One can take advantage of the analytic form of the Green function to efficiently and accurately calculate quantities integrated over the DOS, such as the integrated density of states or the band energy. Finally, one can also take advantage of this analytic representation to describe the electronic properties of alloys, and to investigate the origin of their relative phase stabilities by using perturbation theories in the context of the continued fraction representation of the

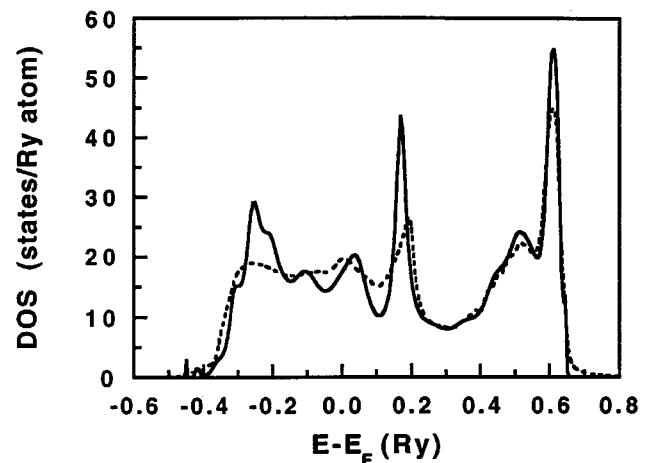


FIG. 12. Same as for Fig. 9 for the bcc-based ternary $Zr_{0.50}Ru_{0.25}Rh_{0.25}$ disordered alloy.

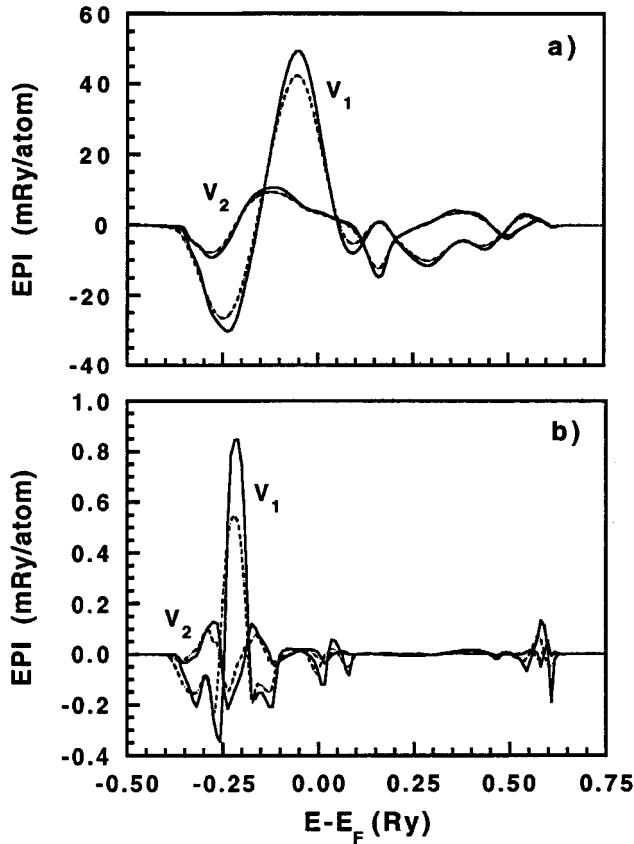


FIG. 13. First and second EPI's for the bcc-based: (a) binary $Zr_{0.5}Rh_{0.5}$ and (b) pseudobinary $Zr_{0.50}(Ru_{0.25}Rh_{0.25})$ disordered alloys as functions of energy (with E_F taken as zero of energy). Results from real-space and k -space calculations are represented by solid lines and dashed lines, respectively.

one-electron Green function, such as the linearized Green function method²⁸ which has been initially proposed for pure metals.

B. Effective pair interactions

As we have seen in Sec. III, once the self-energies and renormalized interactors are defined in terms of continued fraction expansions, and computed with the CPA-extended recursion scheme, it is a simple task to compute the EPI's with a combined OPM-recursion scheme within the ECM. This evaluation does not rely on any numerical integration, and only requires the knowledge of site-diagonal elements of Green functions. This approach has been applied to the calculation of the EPI's for the binary, pseudobinary, and ternary alloys introduced in the previous subsection, and a comparison has been made with the results obtained within the GPM with a standard k -space approach.

Figure 13 shows the most dominant EPI's $V_s^{(2)}$, where s refers to a shell index, for the binary $Zr_{0.5}Rh_{0.5}$ and the pseudobinary $Zr_{0.50}(Ru_{0.25}Rh_{0.25})$ disordered alloys, as functions of energy (with the Fermi energy E_F taken as zero of energy). Both the real-space and k space approaches lead to almost indistinguishable results. Note that the minor differences may be attributed to contributions of self-retracing interactions of higher order which are accounted for in the

ECM and ignored in the GPM, as mentioned in Sec. III A (see also Ref. 10 for further discussion).

In the case of the binary alloy at equiatomic composition, we find that the dominant first and second-neighbor EPI's are positive, with $V_1^{(2)} \gg V_2^{(2)}$. According to the ground-state analysis of the Ising model,²⁹ the ground state is of $B2$ or $CsCl$ -type at this alloy composition, in agreement with the experimental observation of this phase.³⁰ Figure 13 also suggests that by decreasing the number of valence electrons, which can be achieved by replacing for example a fraction of the Rh atoms by Ru atoms, there will be a stronger tendency towards $B2$ order (since the most important contribution to the ordering energy, given by $V_1^{(2)}$, increases by lowering the Fermi energy, i.e., the number of valence electrons).

Similar to what was mentioned in the previous subsection, the calculation of an EPI can be performed very efficiently by minimizing the number of lattice sites visited during the recursion procedure (number corresponding to q levels of continued fraction), while keeping a certain number of sites along each semilinear chain which "dresses" each lattice site (number associated with $p > q$ levels of continued fraction). This property is even better followed in the present calculation, since, implicitly, an EPI is defined as a quantity integrated over the DOS, and is therefore less sensitive to deviations from the most converged determination of the elements of Green functions. For example, the results displayed in Fig. 13 obtained with $p=q=17$ are practically indistinguishable from the ones obtained with $p=10$ and $q=3$. However, note that this property will not only depend on the type of lattice and the range of the SK parameters, but also on the range of the EPI's.

In the case of the pseudobinary alloy, assuming that the Zr atoms fully occupy one of the two sc sublattices which form the bcc lattice, Fig. 13 shows that the first-neighbor EPI (on the sc lattice, which corresponds to the second-neighbor EPI on the bcc lattice) is slightly negative. This would indicate that the Ru and Rh atoms have a tendency to cluster (on this sublattice), but because of the extremely small amplitude of the EPI's at the Fermi energy, it is more likely that these two species will form a solid solution on the sc sublattice while the Zr atoms fully occupy the other sublattice.

Finally, we display in Fig. 14 the most dominant first- and second neighbor EPI's for the three types of pairs, in the case of a bcc-based ternary $Zr_{0.50}Ru_{0.25}Rh_{0.25}$ disordered alloy as a function of energy (with the Fermi energy taken as zero of energy). Note that in the case of higher-order component alloys, one has to define for each combination of two species i and j an EPI, in the same way it is done for a binary alloy, see also Eq. (3.6), in terms of the combination

$$V_s^{(2),ij} = V_s^{ii} + V_s^{jj} - 2V_s^{ij}, \quad (4.6)$$

where s is a shell index. This leads for an alloy with n_c components to the definition of $n_c(n_c - 1)/2$ EPI's per shell index.

Once again, an excellent agreement between real-space and k -space results is achieved. Hence, at the Fermi energy corresponding to this ternary alloy, we find the following hierarchy for the dominant EPI's,

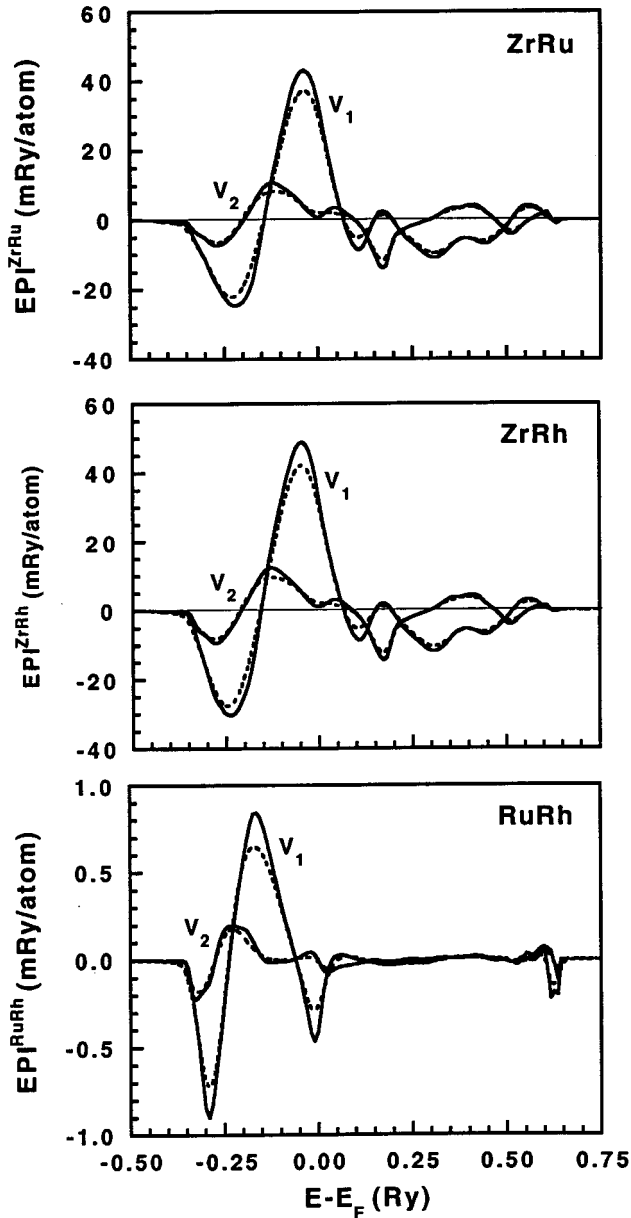


FIG. 14. First ($s=1$) and second ($s=2$) effective pair interactions $V_s^{(2),ij}$, where $ij = \text{ZrRu}$ (top), ZrPd (middle), and RuRh (bottom), for the bcc-based ternary $\text{Zr}_{0.50}\text{Ru}_{0.25}\text{Rh}_{0.25}$ disordered alloy, as functions of energy (with E_F taken as zero of energy).

$$\begin{aligned}
 V_1^{(2),\text{ZrRu}} &\gg V_2^{(2),\text{ZrRu}} > 0, \\
 V_1^{(2),\text{ZrRh}} &\gg V_2^{(2),\text{ZrRh}} > 0, \\
 V_1^{(2),\text{RuRh}} &< 0 \quad \text{and} \quad V_2^{(2),\text{RuRh}} > 0.
 \end{aligned} \quad (4.7)$$

Note also that $V_1^{(2),\text{ZrRu}} \sim V_1^{(2),\text{ZrRh}} \gg |V_1^{(2),\text{RuRh}}|$. A ground-state analysis of the Ising model performed for ternary alloys based on the bcc lattice³¹ with first- and second-neighbor EPI's predicts a tendency towards phase separation in two $B2$ ordered states, ZrRu and ZrRh , as expected from the magnitude and the negative sign of the EPI's involved between Ru and Rh. These results established from the knowledge of the electronic structure properties of the fully random ternary alloy are fully consistent with the previous

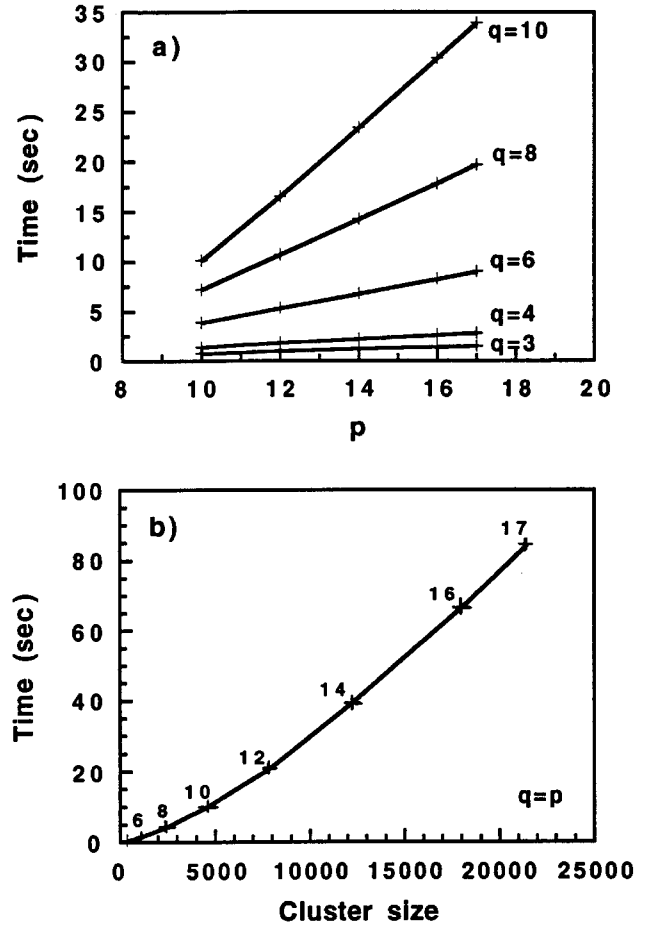


FIG. 15. Execution time (in sec) for computing a DOS as a function of (a) p , for various values of q ; and (b) cluster size, corresponding to various values of $q (=p)$ indicated by the numbers along the curve. The absolute time corresponds to CPU time on a workstation DEC Alpha 250, and the calculations have been performed for a bcc-based binary alloy $\text{Zr}_{0.5}\text{Rh}_{0.5}$.

results found in the case of the pseudobinary alloy. Note that similar results have been obtained and further discussed in the case of the $\text{Zr}_{0.5}(\text{Ru}_{1-c}\text{Pd}_c)_{0.5}$.²⁵

C. Considerations on performance

So far, all the computations have been carried out on a sequential computer, a DEC Alpha workstation 250 with a clock frequency of 266 MHz. A full calculation of the DOS, i.e., for four orbital symmetries, with $q=3$ and $p=10$, on a cluster of 175 sites is performed in a time t_0 of 0.75 sec, to be compared with 85 sec in the case $q=p=17$ which corresponds to a cluster of 21 455 sites on the bcc lattice, for the binary alloy $\text{Zr}_{0.5}\text{Rh}_{0.5}$. The execution time t_1 for one EPI is roughly given by $t_1 \sim 4 \times 9 \times (t_0/4)$, i.e., $9t_0$, where 4 refers to the number of combinations of ij species, and 9 to the number of orbitals peeled within the OPM. Obviously, once the continued fraction expansions of $\sigma(z)$ and $\Delta(z)$ are known, the 4×9 recursions can be performed on a parallel machine with a particle distribution, here 36 particles, among 36 processors, so that perfect load balance between processors can be achieved with an execution time $t_0/4$ on each processor.

Also, note that, at fixed q , i.e., for a fixed number of sites which belong to the real crystal (cluster size), the execution time scales linearly with the “length” of the semilinear chain, or p , as illustrated in Fig. 15(a), as opposed to the execution time versus cluster size (or $q=p$) as shown in Fig. 15(b). This is an important property since the calculation of an interaction within the OPM requires a number of poles and zeros, see Eqs. (3.10) and (3.11) to be accurate. Fortunately the parameter q can be chosen very small while preserving the accuracy for the determination of the DOS, and of any quantity integrated over the DOS such as the band energy or the EPI's, as discussed in the two previous subsections.

V. CONCLUSION

We have shown that, within the tight-binding framework, the CPA equations can be very efficiently solved in real space with the recursion technique. This methodology leads to an accurate description of the electronic structure properties of binary alloys with a straightforward extension to higher-order multicomponent alloys when combined with the configuration sum-space approach. In addition, the configurational contribution to the total energy, as described within the embedded cluster method, can be efficiently and accurately determined in real space, with the orbital-peeling method and the recursion technique, and the codes resulting from this methodology can be ideally implemented on parallel machines with an adequate load balance.

The present formalism, although applied here to alloys with a periodic underlying lattice, is well suited for further developments to address stability and chemical order issues in multi-component alloys with reduced or no symmetry, taking full advantage of the overall real-space description and the continued fraction expansion of the one-electron Green function, and the properties of the configuration sum space. In addition, since the CPA-extended recursion technique is based on the locator formalism, extension of the methodology to account for off-diagonal disorder effects in alloys is straightforward. Preliminary results on these extensions will be discussed in a forthcoming paper. Finally, the recent real-space implementation of the Kubo-Greenwood formulas within tight binding for model systems³² can, and will, be extended to a realistic electronic structure description of alloys with or without periodicity, so that electronic transport and diffusivity as functions of alloy parameters can be studied.

ACKNOWLEDGMENTS

This work was performed under the auspices of the U.S. Department of Energy by the Lawrence Livermore National Laboratory under Contract No. W-7405-ENG-48. Partial support from NATO under Contract No. CRG 941028 is gratefully acknowledged. The authors would like to thank Dr. A. Gonis for fruitful discussions and a careful reading of the manuscript.

-
- ¹P. E. A. Turchi, in *Intermetallic Compounds: Principles and Practice*, edited by J. H. Westbrook and R. L. Fleischer (Wiley, New York, 1995), Vol. 1, Chap. 2, pp. 21–54.
- ²R. Haydock, in *Solid State Physics: Advances in Research and Applications*, edited by H. Ehrenreich, F. Seitz, and D. Turnbull (Academic Press, New York, 1980), Vol. 35, p. 215.
- ³*Recursion Method and its Applications*, edited by D. G. Pettifor and D. L. Weaire, Springer Series in Solid States Sciences Vol. 58 (Springer-Verlag, Berlin, 1985).
- ⁴P. Turchi, F. Ducastelle, and G. Tréglia, *J. Phys. C* **15**, 2891 (1982); G. Grosso, G. Pastori Parravicini, and A. Testa, *Phys. Rev. B* **32**, 627 (1985).
- ⁵O. K. Andersen, O. Jepsen, and M. Sob, in *Electronic Band Structure and its Applications*, edited by M. Yussouff (Springer-Verlag, Berlin, 1987), p. 1.
- ⁶F. Ducastelle and F. Gautier, *J. Phys. F* **6**, 2039 (1976).
- ⁷J. S. Faulkner, *Prog. Mater. Sci.* **27**, 1 (1982), and references cited therein.
- ⁸F. Ducastelle, *Order and Phase Stability in Alloys*, edited by F. R. de Boer and D. G. Pettifor, Cohesion and Structure Series, Vol. 3 (North-Holland, Amsterdam, 1991).
- ⁹A. Gonis, *Green Functions for Ordered and Disordered Systems*, edited by E. van Groesen and E. M. DeJager, Studies in Mathematical Physics Vol. 4 (North-Holland, Amsterdam, 1992).
- ¹⁰A. Gonis, X.-G. Zhang, A. J. Freeman, P. E. A. Turchi, G. M. Stocks, and D. M. Nicholson, *Phys. Rev. B* **36**, 4630 (1987).
- ¹¹J. W. D. Connolly and A. R. Williams, *Phys. Rev. B* **27**, 5169 (1983).
- ¹²N. R. Burke, *Surf. Sci.* **58**, 349 (1976).
- ¹³A. Mookerjee, *J. Phys. C* **6**, 1340 (1973).
- ¹⁴I. Dasgupta, T. Saha, and A. Mookerjee, *Phys. Rev. B* **51**, 3413 (1995).
- ¹⁵H. Shiba, *Prog. Theor. Phys.* **46**, 77 (1971).
- ¹⁶D. Mayou, A. Pasturel, and D. Nguyen Manh, *J. Phys. C* **19**, 719 (1986).
- ¹⁷A. Cordelli, G. Grosso, and G. Pastori Paravicini, *Phys. Rev. B* **44**, 2946 (1991).
- ¹⁸A. Cordelli, G. Grosso, and G. Pastori Paravicini, *Phys. Rev. B* **48**, 11 567 (1993).
- ¹⁹T. Saha, I. Dasgupta, and M. Mookerjee, *J. Phys. Condens. Matter* **6**, L245 (1994); *Phys. Rev. B* **50**, 13 267 (1994).
- ²⁰J. P. Julien and D. Mayou, *J. Phys. (France) I* **3**, 1861 (1993).
- ²¹J. A. Blackman, D. M. Esterling, and N. F. Berk, *Phys. Rev. B* **4**, 2412 (1971).
- ²²A. Gonis and J. W. Garland, *Phys. Rev. B* **16**, 1495 (1977).
- ²³M. O. Robbins and L. M. Falicov, *Phys. Rev. B* **29**, 1333 (1984).
- ²⁴N. Beer and D. G. Pettifor, in *The Electronic Structure of Complex Systems*, Vol. 113 of *NATO Advanced Study Institute, Series B: Physics*, edited by P. Phariseau and W. M. Temmerman (Plenum, New York, 1984), p. 769.
- ²⁵A. Traiber, P. E. A. Turchi, R. M. Waterstrat, and S. M. Allen, *J. Phys., Condens. Matter* **8**, 6357 (1996).
- ²⁶J. C. Slater and G. F. Koster, *Phys. Rev. B* **94**, 1498 (1954).
- ²⁷D. J. Chadi and M. L. Cohen, *Phys. Rev. B* **8**, 5747 (1973).
- ²⁸P. Turchi and F. Ducastelle, in *The Recursion Method and its Applications*, edited by D. G. Pettifor and D. L. Weaire,

- Springer Series in Solid State Sciences Vol. 58 (Springer-Verlag, Berlin, 1985), p. 104.
- ²⁹S. M. Allen and J. W. Cahn, *Acta Metall.* **20**, 423 (1972).
- ³⁰*Binary Alloy Phase Diagrams*, edited by T. B. Massalski (ASM International, Materials Park, OH, 1990), Vols. 1–3.
- ³¹A. J. S. Traiber and S. M. Allen, *Acta Metall. Mater.* **40**, 1403 (1992).
- ³²D. Mayou and S. N. Khanna, *J. Phys. (France) I* **5**, 1199 (1995).